

A NOTE ON QR-BASED MODEL REDUCTION: ALGORITHM, SOFTWARE, AND GRAVITATIONAL WAVE APPLICATIONS*

HARBIR ANTIL[†], DANGXING CHEN[‡], AND SCOTT E. FIELD[§]

Abstract. While the proper orthogonal decomposition (POD) is optimal under certain norms it's also expensive to compute. For large matrix sizes, it is well known that the QR decomposition provides a tractable alternative. Under the assumption that it is rank-revealing QR (RRQR), the approximation error incurred is similar to the POD error and, furthermore, we show the existence of an RRQR with exactly same error estimate as POD. To numerically realize an RRQR decomposition, we will discuss the (iterative) modified Gram Schmidt with pivoting (MGS) and reduced basis method by employing a greedy strategy. We show that these two, seemingly different approaches from linear algebra and approximation theory communities are in fact equivalent. Finally, we describe an MPI/OpenMP parallel code that implements one of the QR-based model reduction algorithms we analyze. This code was developed with model reduction in mind, and includes functionality for tasks that go beyond what is required for standard QR decompositions. We document the code's scalability and show it to be capable of tackling large problems. In particular, we apply our code to a model reduction problem motivated by gravitational waves emitted from binary black hole mergers and demonstrate excellent weak scalability on the supercomputer Blue Waters up to 32,768 cores and for complex, dense matrices as large as 10,000-by-3,276,800 (about half a terabyte in size).

Key words. greedy algorithm, QR decomposition, rank revealing, low-rank approximations, software

AMS subject classifications.

1. Introduction. Algorithms to compute low-rank matrix approximations have enabled many recent scientific and engineering advances. In this CiSE special issue, we summarize the theoretical properties of the most influential low-rank techniques. We also show two of the most popular techniques are algorithmically equivalent and describe a massively parallel code for QR-based model reduction that has been used for gravitational wave applications. This preprint is an expanded, more technical version of the manuscript published in IEEE's Computing in Science & Engineering.

In this paper we consider both practical and theoretical low-rank approximations found by singular value decomposition (SVD) or QR decomposition of a matrix S , presenting error estimates, algorithms and properties of each. Both decompositions can be used, for example, to compute a low-rank approximation to a matrix (a common task in numerical linear algebra) or provide a high-fidelity approximation space suitable for model order reduction (a common task in engineering or approximation theory).

For certain norms an SVD-based approximation is optimal. However, for many large problems the (classical) SVD becomes problematic in terms of its memory footprint, FLOP count, and scalability on many-core machines. By comparison, QR-based model reduction is computationally competitive; it carries a lower FLOP count, is easily parallelized, and has a small inter-process communication overhead, thereby allowing one to efficiently utilize many-core machines. Indeed, for large matrices some

*HA has been supported in part by NSF grant DMS-1521590. SEF has been supported in part by NSF grants PHY-1606654 and the Sherman Fairchild Foundation.

[†]Department of Mathematical Sciences, George Mason University, Fairfax, VA 22030, USA. hantil@gmu.edu,

[‡]Department of Mathematics, University of North Carolina. Chapel Hill, NC 27514, USA. (dangxing@live.unc.edu)

[§]Department of Mathematics. University of Massachusetts, Dartmouth, MA 02747, USA. (sfield@umassd.edu)

SVD algorithms are based on QR decompositions [17]. Furthermore, for certain matrices S , we will show that the SVD and a special class of QR decompositions share similar approximation properties.

We are especially interested in the setting where the snapshot (or “data”) matrix may be too large to load into memory thereby precluding straightforward use of the singular value or, equivalently, a proper orthogonal decomposition (POD). In order to salvage an SVD approach, randomized or hierarchical methods can be used. QR factorizations have long been recognized as an alternative low-rank approximation. For instance the *rank revealing* QR (RRQR) factorization [14, 13, 15, 24] computes a decomposition of a matrix $S \in \mathbb{R}^{N \times M}$ as

$$S\Pi = QR = Q \begin{bmatrix} R_{11} & R_{12} \\ 0 & R_{22} \end{bmatrix}, \quad (1.1)$$

where $Q \in \mathbb{R}^{N \times N}$ is orthogonal, $R_{11} \in \mathbb{R}^{k \times k}$ is upper triangular, $R_{12} \in \mathbb{R}^{k \times (M-k)}$, and $R_{22} \in \mathbb{R}^{(N-k) \times (M-k)}$. The column permutation matrix Π is usually chosen such that $\|R_{22}\|_2$ is small and R_{11} is well-conditioned. This factorization (1.1) was introduced in [24], and the first algorithm to compute it is based on the QR factorization with column pivoting [11]. We also refer to a recent work on this subject [18].

While an RRQR always exists (see Sec. 5.1), it may be computationally challenging to find. We shall consider two specific QR strategies: modified Gram Schmidt (MGS) and a reduced basis method using a greedy strategy (RB-greedy). Although the former algorithm is widely known within the linear algebra community, the latter has become extremely popular in the approximation and numerical analysis communities [7, 19, 10]. We show that finite dimensional versions of these two approaches produce equivalent basis sets and discuss their error estimates. While for a generic S these algorithms may not provide a RRQR, in all practical settings with which we are familiar these algorithms are rank revealing and the resulting RRQR approximation error is of the same order as the SVD/POD. There may be additional advantages when the columns form the basis as opposed to linear combinations over all columns; a typical example is column subset selection [40].

As a rank-revealer, the column pivoted QR decomposition is known to fail on, for example, Kahan’s matrix [29]. A formal fix to this is discussed in [18, Section 4], see also [20] where several related issues were analyzed and the appropriate algorithmic fixes were discussed. Nevertheless, matrices like the Kahan one are rarely (if ever) encountered in model reduction problems. In typical cases, the approximation properties of QR-based model reduction is summarized as follows. The RB-greedy error in Algorithm 3 is given by $\max_{1 \leq i \leq M} \|s_i - Q_k Q_k^T s_i\|_2$ where $s_i \in \mathbb{R}^N$ are columns of S and $Q_k \in \mathbb{R}^{N \times k}$ (see Definition 2.3). The state-of-the-art results presented in [19, 7] provide us an a priori behavior of this error: if the Kolmogorov n -width (best approximation error) decays exponentially with respect to k so does the greedy error. For many model reduction problems, smoothness with respect to parametric variation plays an essential role. For smooth models the n -width (and thus the greedy error) is expected to decay exponentially fast [19, 34].

We will show that MGS is equivalent to RB-greedy (see Proposition 5.3) and derive error estimates for both algorithms. We recall error estimates for the *full* QR decomposition in Theorems 4.1–4.3 and, under the assumption that this decomposition is an RRQR, we show that the underlying error is of same order as POD in the ℓ^2 -norm. Existence of an *optimal* RRQR decomposition is shown. We give a reconstruction strategy in Section 5.2.2, which is cheaper than, but as accurate as,

the POD.

A key contribution of this paper is the development of a publicly available code ¹ that implements the RB-greedy algorithm parallelized with message passing interface (MPI) and OpenMP. Unlike other parallelized QR codes, our software is designed with model reduction in mind and uses a simple interface for easy integration with model-generation codes. Sec. 6 documents the code’s performance for dense matrices with sizes as large as 10^7 -by- 10^4 . Model reduction is sometimes combined with an empirical interpolation method, and we briefly document our codes efficiency in computing empirical interpolants [32, 16] using many thousands of basis. We focus on generating empirical interpolants for the acceleration of gravitational wave parameter inference [6, 2, 37, 12, 33]; the QR-accelerated inference codes have been used in the most recent set of gravitational wave detections [2, 4, 3]. For such large dimensional reduction problems, an efficient, parallelized code [1] running on thousands of cores has proven essential.

The outline of this paper is as follows. In Section 2 we introduce projection based reduced order model (ROM) techniques. We summarize well known facts about POD/SVD-based model reduction in Section 3 such as optimality results and error bounds. Section 4 discusses the *full* QR factorization and the resulting approximation. Section 5 motivates rank revealing QR-based model reduction as a computationally efficient alternative and provides error bounds and comparisons to POD. Two specific QR-based algorithms (MGS and RB-greedy) are considered and compared in Section 5.2.1, and reconstruction technique is presented in Section 5.2.2. Section 6 documents performance and scalability tests of the open-source `greedycpp` code developed in this paper [1].

2. Dimensional reduction techniques. Let us assume we are given M samples $s_1, \dots, s_M \in \mathbb{R}^N$ and an associated snapshot matrix $S = (s_1, \dots, s_M) \in \mathbb{R}^{N \times M}$ whose i^{th} column is s_i . Each s_i corresponds to a realization of an underlying parameterized model: we evaluate the model at selected parameter values and designate the solution as s_i .

Within the setting just described, reduced order models are derived from a low-rank approximation for S . As briefly summarized in this section, the SVD and QR exposes certain kinds of low-rank approximations. We introduce a few definitions.

DEFINITION 2.1 (full SVD). *Given a matrix $S \in \mathbb{R}^{N \times M}$, the full SVD of S is*

$$S = V \Sigma W^T,$$

where $V \in \mathbb{R}^{N \times N}$, $\Sigma \in \mathbb{R}^{N \times M}$, $W \in \mathbb{R}^{M \times M}$. In addition, V and W are orthogonal matrices, and Σ is a diagonal matrix with non-increasing entries, known as singular values. The k^{th} singular value is denoted by σ_k .

From the singular values we define the *ordinary* and *numerical-ranks* of a matrix as follows:

DEFINITION 2.2 (ordinary- and numerical-ranks of S). *Let $S \in \mathbb{R}^{N \times M}$ be a matrix whose singular values $\{\sigma_i\}_{i=1}^M$ are arranged in a decreasing order. Then S is said to have numerical rank k if*

$$\sigma_{k+1} \approx \epsilon_{\text{mach}}$$

where ϵ_{mach} is the machine precision and a standard, or ordinary-rank, if

$$\sigma_{k+1} = 0.$$

¹The code is available at <https://bitbucket.org/sfield83/greedycpp/>.

DEFINITION 2.3 (full QR). *The full QR factorization of $S \in \mathbb{R}^{N \times M}$ is*

$$S\Pi = QR = \begin{bmatrix} Q_k & Q_{N-k} \end{bmatrix} \begin{bmatrix} R_{11} & R_{12} \\ 0 & R_{22} \end{bmatrix}. \quad (2.1)$$

where $Q_k \in \mathbb{R}^{N \times k}$ and $Q_{N-k} \in \mathbb{R}^{N \times (N-k)}$ are orthogonal, $R_{11} \in \mathbb{R}^{k \times k}$ is upper triangular, $R_{12} \in \mathbb{R}^{k \times (M-k)}$, and $R_{22} \in \mathbb{R}^{(N-k) \times (M-k)}$.

The role of a permutation matrix $\Pi \in \mathbb{R}^{M \times M}$ in (2.1) is to swap columns of S and is crucial for achieving QR-based model reduction. Different QR algorithms prescribe different rules for discovering Π . If QR is not pivoted, then we define the permutation matrix as identity.

Of particular interest is the RRQR decomposition. There are several different ways of defining an RRQR, one of them [29, 15] says that the factorization (2.1) is an RRQR if:

DEFINITION 2.4 (RRQR). *Assume $S \in \mathbb{R}^{N \times M}$ has numerical rank k , if*

$$\sigma_{\min}(R_{11}) \gg \|R_{22}\|_2 \approx \epsilon_{\text{mach}}$$

then the factorization $S\Pi = QR$ is called a Rank Revealing QR factorization (RRQR) of S .

From [29, Lemma 1.2] we recall that the following holds for any Π

$$\sigma_k(S) \geq \sigma_{\min}(R_{11}) \quad \text{and} \quad \|R_{22}\|_2 = \sigma_{\max}(R_{22}) \geq \sigma_{k+1}(S),$$

whence Definition 2.4 implies

$$\sigma_{k+1}(S) \leq \|R_{22}\|_2 = \sigma_{\max}(R_{22}) \ll \sigma_{\min}(R_{11}) \leq \sigma_k(S),$$

i.e., Definition 2.4 introduces a large gap between $\sigma_{k+1}(S)$ and $\sigma_k(S)$. Finally, we define an *optimal RRQR* of S as follows:

DEFINITION 2.5 (optimal RRQR). *QR = S\Pi is an optimal RRQR of $S \in \mathbb{R}^{N \times M}$ if*

$$\|S - Q_k Q_k^T S\|_2 = \sigma_{k+1}. \quad (2.2)$$

Projection-based model reduction represents a single column of the matrix, s_i , via orthogonal projection of s_i onto the span of the basis. Approximation errors using an SVD basis, $s_i - V_k V_k^T s_i$, or using a QR basis, $s_i - Q_k Q_k^T s_i$, are considered in the next sections. Throughout this paper we will use V_k to denote a matrix formed by the first k columns of V .

3. Full POD/SVD with error estimates. We first recall the POD problem formulation: A POD computes k orthonormal vectors $v_1, \dots, v_k \in \mathbb{R}^N$ which provide an optimal solution to

$$\epsilon_* := \min_{Y_k \in \mathbb{R}^{N \times k}} \|S - Y_k Y_k^T S\|_*^2 \quad (3.1)$$

where $*$ is either the Frobenius (F) or matrix 2-norm. It is well known that the $*$ -norm solution to (3.1) can be computed by first performing a SVD of $S = V\Sigma W^T$, from which $Y_k = V_k = (v_1, \dots, v_k) \in \mathbb{R}^{N \times k}$ is simply the first k columns of V .

We shall assume, for definiteness, a *full SVD* of S . We will frequently require matrices with zeros in all columns after $k+1$ and shall denote these with a superscript “0”. For example, $V_k V_k^T V := V_k^0$ is V with zeros in columns $k+1$ to N . Using this notation it is easy to see that the POD approximation of S

$$V_k V_k^T S = V_k V_k^T V \Sigma W^T = V_k^0 \Sigma W^T = V \Sigma_k^0 W^T = \sum_{i=1}^k \sigma_i v_i w_i^T \quad (3.2)$$

is exactly a sum of k rank-one matrices, where Σ_k^0 is Σ with zeros in columns $k+1$ to N . This illustrates the close connection of POD with the *partial SVD* factorization $V \Sigma_k^0 W^T$.

3.1. 2-norm and F -norm POD error estimates. We briefly recall standard POD error estimates.

LEMMA 3.1. *Let A and B be two matrices. If A is orthogonal then $\|AB\|_* = \|B\|_*$; if B is orthogonal, then $\|AB\|_* = \|A\|_*$.*

THEOREM 3.2 (POD error estimates). *Given $S \in \mathbb{R}^{N \times M}$ with SVD of $S = V \Sigma W^T$, then*

$$(i) \|S - V_k V_k^T S\|_F^2 = \sum_{j=k+1}^{\min\{M, N\}} \sigma_j^2.$$

$$(ii) \|S - V_k V_k^T S\|_2 = \sigma_{k+1}.$$

Proof. The proof is standard but we recall it here for completeness. By Lemma 3.1 and Equation (3.2)

$$\|S - V_k V_k^T S\|_*^2 = \|V \Sigma - V_k V_k^T V \Sigma\|_*^2 = \|\Sigma - \Sigma_k^0\|_*^2.$$

From the definition of F and 2 norms, we deduce

$$\|\Sigma - \Sigma_k^0\|_F^2 = \sum_{j=k+1}^{\min\{m, N\}} \sigma_j^2, \quad \|\Sigma - \Sigma_k^0\|_2 = \sigma_{k+1},$$

which completes the proof. \square

From Theorem 3.2, errors measured in the F -norm require computation of all singular values, which can be expensive. Using the 2-norm requires only the first $k+1$ singular values, which motivates a choice of $\sigma_{k+1} < \tau$ to control the approximation error τ in Algo. 1. In practice, we always choose τ larger than machine precision.

Algorithm 1 POD

- 1: **Input:** Snapshot matrix $S = (s_1, \dots, s_M) \in \mathbb{R}^{N \times M}$ and tolerance $\tau > 0$
 - 2: **Output:** $V_k = (v_1, \dots, v_k) \in \mathbb{R}^{N \times k}$
 - 3: Compute the singular value decomposition $S = V \Sigma W^T$.
 - 4: Find smallest index k such that the singular values satisfy $\sigma_{k+1} < \tau$.
 - 5: Return the first k columns $V_k = (v_1, \dots, v_k) \in \mathbb{R}^{N \times k}$ of V .
-

4. Full QR with error estimates. In Theorem 3.2 we showed that POD provides the best rank k $*$ -norm approximation to the snapshot matrix S . In Theorem 4.1 we will see that under the assumption that the decomposition is an RRQR (according to Def. 2.4) the resulting approximation error using *full* QR factorization is of the same order as POD-based approximation error. In Section 4.1 we will first discuss the $*$ -norm error estimates and we conclude with max-norm error estimates in Section 4.2. Note that a QR decomposition always exists but need not be unique [39].

4.1. 2-norm and F -norm error estimates. We define the QR-based error for the decomposition (2.1) as

$$\epsilon_*^{QR}(\Pi) := \|S\Pi - Q_k Q_k^T S\Pi\|_* = \|S - Q_k Q_k^T S\|_*, \quad (4.1)$$

where $*$ could be either 2-norm or F -norm. The QR-based approximation error depends on the permutation matrix implicitly through Q_k . To avoid extra notation, we sometimes omit writing $S\Pi$ and assume S is already pivoted when it is clear from context.

Let

$$R = \overline{V}\Sigma\overline{W}^T, \quad (4.2)$$

be the SVD of R where we have added over-bars to make a clear distinction with the SVD of S and, recall, that S and R have the same singular value spectrum (hence $\overline{\Sigma} = \Sigma$). Furthermore $\overline{V} \in \mathbb{R}^{N \times N}$, $\overline{W} \in \mathbb{R}^{M \times M}$ and $\Sigma \in \mathbb{R}^{N \times M}$. Let

$$Q_k^0 := Q_k Q_k^T Q \quad (4.3)$$

be Q with zeros in columns from $k+1$ to N , $\overline{V}_{k,0}$ is \overline{V} with zeros from rows $k+1$ to N , and $\overline{V}_{N-k,0}$ is \overline{V} with zeros from rows 1 to k . Observe that

$$Q_k^0 \overline{V} = Q \overline{V}_{k,0}. \quad (4.4)$$

THEOREM 4.1 (full QR $*$ -norm error estimate). *Let $Q_k \in \mathbb{R}^{N \times k}$ denote the first k columns of Q , then*

$$\epsilon_*^{QR}(\Pi) = \|S - Q_k Q_k^T S\|_* = \|\overline{V}_{N-k,0} \Sigma\|_* = \|R_{22}\|_*, \quad (4.5)$$

where $*$ is either 2-norm or F -norm. A proof can be found in Ref. [13]

Proof. To show the first equality, we use Lemma 3.1, (4.2), and (4.3), we deduce

$$\begin{aligned} \|S - Q_k Q_k^T S\|_* &= \|QR - Q_k Q_k^T QR\|_* = \|QR - Q_k^0 R\|_* \\ &= \|Q\overline{V}\Sigma\overline{W}^T - Q_k^0 \overline{V}\Sigma\overline{W}^T\|_* = \|Q\overline{V}\Sigma - Q_k^0 \overline{V}\Sigma\|_*. \end{aligned}$$

Invoking (4.4), we obtain

$$\|S - Q_k Q_k^T S\|_* = \|Q\overline{V}\Sigma - Q\overline{V}_{k,0}\Sigma\|_* = \|(\overline{V} - \overline{V}_{k,0})\Sigma\|_* = \|\overline{V}_{N-k,0}\Sigma\|_*,$$

which proves the first equality in (4.5).

The proof of the second equality is similar to the proof of Theorem 3.2, we readily obtain

$$\|S - Q_k Q_k^T S\|_* = \|QR - Q_k^0 R\|_* = \|R_{22}\|_*,$$

the last equality naturally comes out as R upper triangular. Thus, we conclude. \square

REMARK 4.2. Invoking the optimality of POD, we notice that $\|S - V_k V_k^T S\|_* \leq \|S - Q_k Q_k^T S\|_*$. Assuming that QR is RRQR (according to Def. 2.4) and employing Theorem 4.1 we notice that the approximation error of the *full* QR and POD are of the same order.

4.2. Max-norm error estimate. We define the QR-based approximation error in the max-norm as

$$\epsilon_{\max}^{QR}(\Pi) := \max_{1 \leq i \leq M} \|s_i - Q_k Q_k^T s_i\|_2, \quad (4.6)$$

where, for vectors, $\|\cdot\|_2$ is the usual Euclidean norm. Measured in the max-norm, the QR-based approximation error is given by the following result.

THEOREM 4.3 (full QR max-norm error estimate). *Let r_i be the i -th column of R and \tilde{r}_i be a subvector of r_i from row $k+1$ to N . Then the approximation error for any given s_i is*

$$\|s_i - Q_k Q_k^T s_i\|_2 = \|\tilde{r}_i\|_2, \quad i = 1, \dots, M,$$

whence $\epsilon_{\max}^{QR} = \max_{1 \leq i \leq M} \|\tilde{r}_i\|_2$.

Proof. Invoking Lemma 3.1 and Equation (4.3), we deduce

$$\|s_i - Q_k Q_k^T s_i\|_2 = \|Q r_i - Q_k Q_k^T Q r_i\|_2 = \|Q r_i - Q_k^0 r_i\|_2 = \|\tilde{r}_i\|_2,$$

thus we conclude. \square

COROLLARY 4.4. *The following relation between the $*$ and max norm estimates for QR holds*

$$\epsilon_{\max}^{QR} \leq \epsilon_*^{QR}.$$

Proof. Invoking Theorem 4.1 and Theorem 4.3 and the fact that \tilde{r}_i is the submatrix of R_{22} , we conclude

$$\max_{1 \leq i \leq M} \|\tilde{r}_i\|_* \leq \|R_{22}\|_*,$$

which is due to the fact that the norm of a submatrix is less than the norm of matrix it embedded in. \square

5. Specific QR algorithms. The goal of this section is to discuss different QR decomposition strategies (that is to say, the pivoting strategy) useful for low-rank approximation. We first consider the *optimal* RRQR whose 2-norm error estimates exactly match the POD error estimates (see Theorem 3.2). Next we consider *practical* RRQR algorithms which are implementable. For the *practical* RRQR, in Section 5.2, we will discuss two algorithms: modified Gram-Schmidt (MGS) with pivoting and a reduced basis method using a greedy approach (RB-greedy). We show that these methods are in fact equivalent in certain settings. We will derive the error estimates and furnish FLOP counts. In Section 5.2.2 we discuss a QR-reconstruction strategy with error estimates similar to POD.

5.1. Optimal RRQR. In this section we show that an optimal QR-based approximation exists (although its not necessarily unique). We will provide a constructive proof. We begin by computing the SVD of S as

$$\begin{aligned} S = V \Sigma W^T &= \begin{bmatrix} V_k & V_{N-k} \end{bmatrix} \begin{bmatrix} \Sigma_k & 0 \\ 0 & \Sigma_{N-k, M-k} \end{bmatrix} \begin{bmatrix} W_k^T \\ W_{M-k}^T \end{bmatrix} \\ &= V_k \Sigma_k W_k^T + V_{N-k} \Sigma_{N-k, M-k} W_{M-k}^T. \end{aligned} \quad (5.1)$$

In addition, let

$$\mathcal{Q}\mathcal{R} = \Sigma_k W_k^T, \quad (5.2)$$

be a QR factorization of $\Sigma_k W_k^T$. Finally, we set

$$Q_k = V_k \mathcal{Q}. \quad (5.3)$$

We will prove that such a Q_k will lead to the *optimal* RRQR according to Def. 2.4.

THEOREM 5.1 (existence of optimal RRQR and equivalence to POD error). *Let $S \in \mathbb{R}^{N \times M}$, then an optimal RRQR (according to Def. 2.4) of S exists, with*

$$Q = [Q_k \quad Q_{N-k}] \quad \text{and} \quad R = \begin{bmatrix} \mathcal{R} \\ 0 \end{bmatrix}, \quad (5.4)$$

where \mathcal{R} and Q_k are defined in (5.2) and (5.3) respectively and $Q_{N-k} \in \mathbb{R}^{N \times (N-k)}$ is defined such that $Q^T Q = I$. The following estimate holds

$$\|S - Q_k Q_k^T S\|_2 = \|S - V_k V_k^T S\|_2 = \sigma_{k+1}. \quad (5.5)$$

where V_k is as defined in Theorem 3.2.

Proof. The proof is constructive. Using the SVD of S from (5.1), it is not difficult to see that

$$\|S - V_k \Sigma_k W_k^T\|_2 = \sigma_{k+1}. \quad (5.6)$$

Next we use (5.3), (5.1), and invoke the orthogonality of V to yield

$$\begin{aligned} \|S - Q_k Q_k^T S\|_2 &= \|S - V_k \mathcal{Q} \mathcal{Q}^T V_k^T S\|_2 \\ &= \|S - V_k \mathcal{Q} \mathcal{Q}^T V_k^T (V_k \Sigma_k W_k^T + V_{N-k} \Sigma_{N-k, M-k} W_{M-k}^T)\|_2 \\ &= \|S - V_k \mathcal{Q} \mathcal{Q}^T \Sigma_k W_k^T\|_2. \end{aligned}$$

Notice that $\mathcal{Q} \mathcal{Q}^T \Sigma_k W_k^T = \mathcal{Q} \mathcal{Q}^T \mathcal{Q} \mathcal{R} = \mathcal{Q} \mathcal{R} = \Sigma_k W_k^T$, where we have used (5.1), we arrive at

$$\|S - Q_k Q_k^T S\|_2 = \|S - V_k \Sigma_k W_k^T\|_2 = \sigma_{k+1},$$

therefore (5.6) in conjunction with Theorem 3.2 enables us to obtain the asserted equality (5.5). \square

We do not offer an efficient algorithm to calculate the *optimal* RRQR other than to first calculate a potentially expensive SVD as in proof. Notice that in this case the optimal RRQR's permutation matrix Π is the identity. In particular, the QR factorization constructed in the proof does not arise from the QR pivoting strategies of Sec. 5.2, and to the best of our knowledge the matrix Q_k cannot in general be constructed as a column subset of S .

The estimate in (5.5) states that 2-norm error in POD (Theorem 3.2) is same as the optimal RRQR. We reemphasize that, although the proof above is constructive, it does not provide a numerical recipe to compute QR factorization. This is the subject of next section.

COROLLARY 5.2 (optimal RRQR and ordinary k -rank matrix). *If $S \in \mathbb{R}^{N \times M}$ has an ordinary rank k then under the assumptions of Theorem 5.1, $S = QR$ with Q and R defined in (5.4).*

Proof. Using (5.2) and (5.3) we first notice that

$$V_k \Sigma_k W_k^T = V_k \mathcal{Q} \mathcal{R} = Q_k R = QR.$$

Since S has ordinary rank k therefore $\sigma_{k+1} = 0$, invoking (5.6) we obtain the assertion. \square

5.2. Practical RRQR. This section is devoted to two algorithms that aim to compute an RRQR. Algorithm 2 is the modified Gram-Schmidt (MGS) with pivoting [25]. Algorithm 3 is a particular flavor of the (by now) standard reduced basis (RB)-greedy algorithm [7, 19, 10]. RB-greedy is a popular tool employed in the construction of model reduction schemes for parameterized partial differential equations. We present each algorithm in their standard presentation, and in Proposition 5.3 show these algorithms to be equivalent when the snapshots s_i are elements of an N -dimensional Euclidean vector space. Theorem 4.3 and Corollary 5.6 motivate the choice of stopping criteria, which relies on diagonal entries of R being non-increasing. This aspect is discussed in Corollary 5.6.

5.2.1. Equivalence of the MGS and RB-greedy algorithms. The MGS with pivoting and RB-greedy algorithms are as follows:

Algorithm 2 MGS with pivoting	Algorithm 3 RB-greedy
1: Input: $S = (s_1, \dots, s_M)$, $\tau > 0$	1: Input: $S = (s_1, \dots, s_M)$, $\tau > 0$
2: Output: $Q_k = (q_1, \dots, q_k)$	2: Output: $Q_k = (q_1, \dots, q_k)$
3: Set $V = S$ and $k = 1$	3: Set $k = 0$
4: Set $R(1, 1) = \max_j \ V(:, j)\ _2$	4: Define $\hat{\sigma}_0(s_i) = \ s_i\ _2$
5: while $R(k, k) > \tau$ do	5: $j(0) = \arg \sup_i \hat{\sigma}_0(s_i)$
6: $i = \arg \max_j \ V(:, j)\ _2$	6: Define $\hat{\sigma}_0 = \hat{\sigma}_0(s_{j(0)})$
7: $\Pi(k, i) = 1$	7: $q_1 = s_{j(0)} / \ s_{j(0)}\ _2$
8: $R(k, k) = \ V(:, i)\ _2$	8: while $\hat{\sigma}_k \geq \tau$ do
9: $Q(:, i) = V(:, i) / R(k, k)$	9: $k = k + 1$
10: for $j = k + 1$ to M do	10: $\hat{\sigma}_k(s_i) = \ s_i - Q_k Q_k^T s_i\ _2 \quad \forall s_i \in S$
11: $R(k, j) = Q(:, k)^T V(:, j)$	11: $j(k) = \arg \sup_i \hat{\sigma}_k(s_i)$
12: $V(:, j) = V(:, j) - R(k, j) Q(:, k)$	12: $\hat{\sigma}_k = \hat{\sigma}_k(s_{j(k)})$
13: end for	13: $q_{k+1} = s_{j(k)} - Q_k Q_k^T s_{j(k)}$
14: $k = k + 1$	14: $q_{k+1} := q_{k+1} / \ q_{k+1}\ _2$
15: end while	15: end while

PROPOSITION 5.3. *For a matrix $S \in \mathbb{R}^{N \times M}$, the RB-greedy Algo. 3 is equivalent to the MGS with column pivoting Algo. 2. Moreover, the diagonal entries of R are non-increasing, i.e.,*

$$R(1, 1) \geq R(2, 2) \geq \dots \geq R(M, M) \geq 0, \quad (5.7)$$

Proof. It is sufficient to show their pivoting strategies are equivalent. In Algo. 3, the k th column pivot is

$$j(k) = \arg \max_i \|s_i - \sum_{j=1}^{k-1} q_j^T s_i q_j\|_2.$$

For MGS with column pivoting Algo. 2 we have

$$\arg \max_i \|v_i^{(k)}\|_2,$$

where $v_i^{(k)}$ is defined from a recurrence relation

$$v_i^{(k)} \leftarrow \zeta := v_i^{(k)} - q_k^T v_i^{(k)} q_k, \quad v_i^{(1)} = s_i.$$

Thus using the orthogonality of q_k we obtain

$$\zeta = v_i^{(1)} - \sum_{j=1}^{k-1} q_j^T v_i^{(1)} q_j = s_i - \sum_{j=1}^{k-1} q_j^T s_i q_j$$

Hence, the selection of pivots

$$\arg \max_i \|s_i - \sum_{j=1}^{k-1} q_j^T s_i q_j\|_2 = \arg \max_i \|v_i^{(k)}\|_2,$$

are equivalent. \square

REMARK 5.4. As presented, the MGS with pivoting carries a greater memory overhead. In terms of operation counts the MGS steps 6 and 12 are dominant, requiring $2N(M-j+1)$ and $4N(M-j)$ FLOPs at iteration j . Then the total count is

$$\sum_{j=1}^k (4N)(M-j) + 2N(M-j-1) \approx \sum_{i=1}^k 6NM - \sum_{j=1}^k (6Nj) = 6kNM - 3Nk^2, \quad (5.8)$$

after k steps. The RB-greedy's dominant cost is the pivoting step 10, where, after k iterations, the accumulated FLOP count is

$$\sum_{i=1}^k (3N(i-1) + N + 2N)M = \sum_{i=1}^k 3NMi \approx \frac{3}{2}k^2NM. \quad (5.9)$$

REMARK 5.5. These algorithms may be modified to improve memory overhead, FLOP counts, or conditioning. For very large problems the dominant FLOP count of Algo. 3 can be dramatically reduced if one stores the projections $Q_k Q_k^T s_i$ from each previous step; this would essentially amount to storing a matrix V as is done in the MGS with pivoting. Furthermore, the naive implementation of the classical Gram-Schmidt procedure can lead to a numerically ill-conditioned algorithm. To overcome this one should use well-conditioned orthogonalization algorithms such as the iterated Gram-Schmidt [23, 28, 36] or Householder reductions. Our implementation of Alg. 3 uses Hoffmann's iterated Gram-Schmidt [28] which maintains orthogonality for extremely large basis sets [21]. We are unaware of results which characterize the preservation of the subspace spanned by the original vectors, but for many approximation-driven applications this is not strictly necessary.

The proof shows their pivoting strategies are equivalent. Having demonstrated the (finite dimensional) equivalence of Algorithms 2 and 3, we now discuss their properties. Recall that diagonal components of R are non-increasing. The following result, which motivated the stopping criterion in Algo. 2, shows how the diagonal entries of R are closely connected with the max-norm approximation error used in Algorithm 3 (see also Theorem 4.3).

COROLLARY 5.6. *The stopping criterion used in Algorithms 2 and 3 fulfills*

$$\max_{1 \leq i \leq M} \|s_i - Q_k Q_k^T s_i\|_2 = R(k+1, k+1).$$

Proof. Theorem 4.3 exactly characterizes the error $\|\tilde{r}_i\|_2$. Then using the definition of $R(k+1, j)$, $j = 1, \dots, M$ it is not difficult to see that

$$\|\tilde{r}_i\|_2 \leq R(k+1, k+1), \quad 1 \leq i \leq M.$$

In addition, we pick $R(k+1, k+1)$ such that

$$R(k+1, k+1) = \max_{1 \leq i \leq M} \|S(:, i) - \sum_{j=1}^k Q(:, j)^T S(:, i) Q(:, j)\|_2,$$

and since the diagonal entries of R are nonincreasing, we obtain

$$R(k+1, k+1) \leq R(k, k) = \max_{1 \leq i \leq M} \|S(:, i) - \sum_{j=1}^{k-1} Q(:, j)^T S(:, i) Q(:, j)\|_2$$

Then the estimate follows after using Theorem 4.3. \square

We next derive a representation of the estimate in Corollary 5.6 in terms of the singular values of S .

COROLLARY 5.7. *Let $S \in \mathbb{R}^{N \times M}$ then*

$$\max_{1 \leq i \leq M} \|s_i - Q_k Q_k^T s_i\|_2 = \left(\prod_{i=1}^{k+1} \sigma_i \right) / \left(\prod_{i=1}^k R(i, i) \right).$$

Proof. Denote by S_{k+1} the first $k+1$ columns of S . Taking QR decomposition of S_{k+1} , we obtain

$$S_{k+1} = QR, \quad Q \in \mathbb{R}^{N \times (k+1)}, \quad R \in \mathbb{R}^{(k+1) \times (k+1)},$$

yielding $\det(S_{k+1}) = \det(R)$. Since $\det(S_{k+1}) = \prod_{i=1}^{k+1} \sigma_i$ and $\det(R) = \prod_{i=1}^{k+1} R(i, i)$, using Corollary 5.6 we arrive at the assertion. \square

5.2.2. A reconstruction approach to QR. We recall that the POD algorithm (1) generates the optimal 2-norm basis (see Theorem 3.2). The goal of this section is to augment the QR with a reconstruction technique such that resulting approximation of S is as accurate as POD, however the algorithm is cheaper than performing an SVD. We note that our method shares some similarities with those algorithms that perform QR decompositions as a precursor to finding the SVD (e.g. [17, 39]).

THEOREM 5.8. *Given $S \in \mathbb{R}^{N \times M}$ with ordinary rank k , if $X = Q\bar{V}$, then $X_k = Q_k \mathcal{V}$, and*

$$\|S - X_j X_j^T S\|_2 = \sigma_{j+1} = \|S - Q_j Q_j^T S\|_2 = \|S - V_j V_j^T S\|_2, \quad 1 \leq j \leq k.$$

Proof. Since S has ordinary rank k , using Corollary 5.2

$$R = \begin{bmatrix} R_{11} & R_{12} \\ 0 & 0 \end{bmatrix} = \bar{V} \Sigma \bar{W}^T.$$

Let $R = \bar{V} \Sigma \bar{W}^T$ be the SVD of R and

$$\mathcal{V} \Sigma_{k, M} \mathcal{W}^T = \begin{bmatrix} R_{11} & R_{12} \end{bmatrix},$$

be *full SVD* of $\begin{bmatrix} R_{11} & R_{12} \end{bmatrix}$, where $\mathcal{V} \in \mathbb{R}^{k \times k}$, $\Sigma_{k,M} \in \mathbb{R}^{k \times M}$, and $\mathcal{W} \in \mathbb{R}^{M \times M}$. Then

$$R = \begin{bmatrix} R_{11} & R_{12} \\ 0 & 0 \end{bmatrix} = \bar{V} \Sigma \bar{W}^T = \begin{bmatrix} \mathcal{V} & 0 \\ 0 & \tilde{\mathcal{V}} \end{bmatrix} \begin{bmatrix} \Sigma_{k,M} \\ 0 \end{bmatrix} \mathcal{W}^T,$$

where $\tilde{\mathcal{V}} \in \mathbb{R}^{(N-k) \times (M-k)}$ is an arbitrary orthogonal matrix. Defining

$$X = Q \bar{V} = \begin{bmatrix} Q_k & Q_{N-k} \end{bmatrix} \begin{bmatrix} \mathcal{V} & 0 \\ 0 & \tilde{\mathcal{V}} \end{bmatrix} = \begin{bmatrix} Q_k \mathcal{V} & Q_{N-k} \tilde{\mathcal{V}} \end{bmatrix}$$

leads to

$$X_j = Q_k \mathcal{V}_j, \quad \text{for } 1 \leq j \leq k.$$

We now show that $\|S - X_j X_j^T S\|_2 = \sigma_{j+1}$ for $1 \leq j \leq k$, the other estimate is due to Theorem 5.1. Recalling $S = QR$ and $R = \bar{V} \Sigma \bar{W}^T$, we deduce

$$\begin{aligned} \|S - X_j X_j^T S\|_2 &= \|X \Sigma \bar{W}^T - X_j X_j^T X \Sigma \bar{W}^T\|_2 = \|X \Sigma - X_j^0 \Sigma\|_2 \\ &= \|X \Sigma - X \Sigma_j\|_2 = \|\Sigma - \Sigma_j^0\|_2 = \sigma_{j+1} = \|S - V_j V_j^T S\|_2, \end{aligned}$$

where X_j^0 is X with zeros in columns $j+1$ to N and the last equality is due to Theorem 3.2(ii). \square

With this motivation, we introduce the following algorithm for a matrix $S \in \mathbb{R}^{N \times M}$ of *numerical rank* k .

Algorithm 4 Reconstruction Algorithm

- 1: **Input:** Samples $S = (s_1, \dots, s_M) \in \mathbb{R}^{N \times M}$, tolerance $\tau_1, \tau_2 > 0$
 - 2: **Output:** $X_k = (x_1, \dots, x_k) \in \mathbb{R}^{N \times k}$
 - 3: Perform a partial j -term MGS with pivoting of S stopping whenever $|R(j, j)| < \tau_1$
 - 4: Let $S = Q_j R(1 : j, 1 : M)$ be the result of step 3
 - 5: Perform an SVD $\mathcal{V} \Sigma \mathcal{W}^T = R(1 : j, 1 : M)$
 - 6: Find $k \in \{1, \dots, j\}$ such that $\sigma_{k+1} < \tau_2 < \sigma_k$
 - 7: Return $X_k = Q_k \mathcal{V}(1 : k, 1 : k)$
-

REMARK 5.9. Computational cost of step 3 is $\mathcal{O}(Mj^2 + Nj^2)$, which is less than the MGS with pivoting cost $\mathcal{O}(jNM)$ given that $j \ll N$. Steps 4-5 enrich the basis: generally speaking, the diagonal entry of R decrease slower than the singular values, and so we employ the SVD basis for improved accuracy.

Next, we give an error estimate for the Reconstruction algorithm. To this end we write $S = S_1 + S_2$, such that

$$S_1 = \begin{bmatrix} Q_k & Q_{N-k} \end{bmatrix} \begin{bmatrix} R_{11} & R_{12} \\ 0 & 0 \end{bmatrix}, \quad S_2 = \begin{bmatrix} Q_k & Q_{N-k} \end{bmatrix} \begin{bmatrix} 0 & 0 \\ 0 & R_{22} \end{bmatrix},$$

where we have assumed that the *full QR* of $S = QR$. In addition, let

$$S_1 = V_1 \Sigma_1 W_1^T, \quad S_2 = V_2 \Sigma_2 W_2^T$$

be the *full SVD* of S_1, S_2 with singular values $\sigma(S_1)_j, \sigma(S_2)_\ell$.

LEMMA 5.10. Let $S \in \mathbb{R}^{N \times M}$ has numerical rank k and if at k^{th} step in Algo. 4 $X_k = Q_k \mathcal{V}_j$, then

$$\begin{aligned} \|S - V_j V_j^T S\|_2 &\leq \|S - X_j X_j^T S\|_2 \\ &\leq \|S_1 - X_j X_j^T S_1\|_2 + \|R_{22}\|_2, \quad \text{for } 1 \leq j \leq k. \end{aligned}$$

Proof. The first inequality follows immediately due to the optimality of the POD. To derive the second inequality we use $S = S_1 + S_2$ and readily obtain

$$\begin{aligned} \|S - X_j X_j^T S\|_2 &= \|S_1 - X_j X_j^T S_1 + S_2 - Q_k \mathcal{V}_j \mathcal{V}_j^T Q_k^T S_2\|_2 \\ &\leq \|S_1 - X_j X_j^T S_1\|_2 + \|(I - Q_k \mathcal{V}_j \mathcal{V}_j^T Q_k^T) S_2\|_2. \end{aligned}$$

Using the definition of S_2 we obtain

$$\|S - X_j X_j^T S\|_2 \leq \|S_1 - X_j X_j^T S_1\|_2 + \|I - Q_k \mathcal{V}_j \mathcal{V}_j^T Q_k^T\|_2 \|R_{22}\|_2.$$

As $Q_k \mathcal{V}_j \mathcal{V}_j^T Q_k^T$ is a projector, hence (see [41, 16, 38]) we obtain

$$\|I - Q_k \mathcal{V}_j \mathcal{V}_j^T Q_k^T\|_2 = \|Q_k \mathcal{V}_j \mathcal{V}_j^T Q_k^T\|_2,$$

thus we conclude. \square

THEOREM 5.11. Under the assumption of Lemma 5.10, for $1 \leq j \leq k$, the following estimate holds

$$\begin{aligned} \|S - V_j V_j^T S\|_2 &\leq \|S - X_j X_j^T S\|_2 \leq \|S_1 - Q_j Q_j^T S_1\|_2 + \|R_{22}\|_2 \\ &= (\sigma_1)_{j+1} + \|R_{22}\|_2. \end{aligned} \quad (5.10)$$

Proof. Recall that

$$S_1 = \begin{bmatrix} Q_k & Q_{N-k} \end{bmatrix} \begin{bmatrix} R_{11} & R_{12} \\ 0 & 0 \end{bmatrix}$$

In view of Lemma 5.10, it is sufficient to realize the result of Theorem 5.8 for S_1 . The proof follows exactly the same way as in Theorem 5.8 and is omitted for brevity. \square

REMARK 5.12 (full QR and reconstruction). For the full QR, we recall that

$$\|S - Q_k Q_k^T S\|_2 = \|QR - Q_k^0 R\|_2 = \|R_{22}\|_2.$$

which is sharper than the reconstruction estimator in (5.10). However, we emphasize that the bound in (5.10) is an estimate and, in addition, the reconstruction algorithm is tractable for large matrix sizes.

REMARK 5.13 (POD and reconstruction). We note that the error bound in (5.10) has two contributions. If $\|R_{22}\|_2$ is of order ϵ_{mach} then the reconstruction (5.10) and POD (Theorem 3.2) error behave similarly.

6. Large-scale QR+DEIM code for model reduction.

6.1. Overview. We now describe an implementation of the greedy algorithm 3 for finding a column-pivoted QR decomposition of a complex-valued, dense matrix. Our publicly available code `greedycpp` [1] has been developed over the past 3 years and has been applied to a variety of production-scale problems. For example, it has been used to build reduced order quadrature rules [6], which can be used to accelerate Bayesian inference studies [12, 37] and provide low-latency parameter estimation (see the supplemental material of Ref. [5]).

As is typical in model reduction applications, given a model M , we shall interpret the column $s_i = M(\mathbf{x}; \nu_i)$ as stemming from the model’s evaluation at a parameter value ν_i and the rows as the evaluations on a grid discretizing the relevant independent variable \mathbf{x} . Alg. 3 identifies the specially selected columns (the pivots) whose span is the reduced model (i.e. basis) space. Our code allows the user to set an approximation error threshold (τ in algorithms 3 and 2) such that, according to Corollary 5.6, guarantees all columns s_i satisfy $\|s_i - Q_k Q_k^T s_i\|_2 < \tau$.

In addition to the dimensional reduction feature, the code also selects a set of empirical interpolation (EI) nodes using a fast algorithm (see Alg. 5 of Ref. [6]) and performs out-of-sample validation of the resulting basis and empirical interpolant. The basis, pivots, and EI nodes can be exported to different file formats including ordinary text, (GSL) binary, and NumPy binary. The code’s simple interface allows any model written in the C/C++ language to be used. Supporting scripts and input files allow for control over the run context. The code can also perform basis validation on quadrature grids that differ from the one used to form S and automatically enrich the basis by iterative refinement [37].

While there has long been an interest in designing efficient parallel algorithms of column pivoting QR factorization, as far as production-scale publicly available codes, however, we are only aware of the (Sca)LAPACK routines. Furthermore, because (Sca)LAPACK is a general purpose linear algebra library, it is insufficient for many model-reduction-type tasks, which is a key reason why we pursued our own implementation. Finally, we note that because column pivoting limits potential parallelism in the QR factorization [22], algorithmic design remains an area of active research [18]. Earlier works proposed BLAS-3 versions of a parallelized algorithm [35] and communication-avoiding local pivoting strategies [8].

6.1.1. Gravitational wave model. We briefly describe the particular model used to form our snapshot matrix S . We use the IMRPhenomPv2 model [27] [27, 30, 31] of gravitational waves emitted by two merging binary black holes. The model is implemented as part of the publicly available LIGO Analysis Library (available, e.g., at <https://github.com/lscsoft/lalsuite>). Our code fills the matrix S by calls to the IMRPhenomPv2 model without any file I/O. The parameter values that define S are distributed among the different MPI processes, and each process is responsible for forming a “slice” of S over a subset of columns. This strategy is useful for computationally-intensive models.

6.1.2. Serial code. Pivoted QR naturally decomposes into two parts, a *pivot search* followed by *orthogonalization*. Consider Alg. 3 at iteration k . The pivot search proceeds by computing all M local error residuals $\hat{\sigma}_k(s_i)$ and finding $J = \arg \sup_i \hat{\sigma}_k(s_i)$. The J^{th} column, s_J , is the one to be pivoted, and an orthogonalized s_J becomes the next column of Q .

Due to the orthogonality of the basis vectors, the relationship

$$Q_k Q_k^T s_i = Q_{k-1} Q_{k-1}^T s_i + q_k q_k^T s_i, \quad (6.1)$$

can be exploited to yield constant complexity at each iteration provided we retain information from the previous iteration, namely $Q_{k-1}Q_{k-1}^T s_i$. We neither store this vector (which would increase the algorithm’s memory footprint) nor replace the columns of S (which requires additional operations of order N). Notice that

$$\|s_i - Q_k Q_k^T s_i\|_2^2 = \|s_i\|_2^2 - \sum_{j=0}^k c_j c_j^*, \quad (6.2)$$

where $c_j = q_j^T s_i$ is the inner product between s_i and the j^{th} basis. The relationship (6.1) becomes

$$\hat{\sigma}_k^2(s_i) = \|s_i\|_2^2 - \left[\sum_{j=0}^{k-1} c_j c_j^* + c_k c_k^* \right], \quad (6.3)$$

and, furthermore, the square-root need not be taken in order to identify the next pivot. To avoid catastrophic cancellation error, we store values for both $\|s_i\|$ and $\sum_{j=0}^{k-1} c_j c_j^*$. As the sum consists of non-negative terms, the update $\sum_{j=0}^{k-1} c_j c_j^* \rightarrow \sum_{j=0}^k c_j c_j^*$ is well-conditioned. The j^{th} pivot search has a constant complexity with an asymptotic FLOP count of $\mathcal{O}(2MN)$. Fig. 6.1(a) (left) plots the scaled time of T_j^{pivot}/N with the iteration index j for different values of N .

Next, the newly selected pivot column is orthogonalized with respect to the existing basis set to yield the next basis q_k , which, in turn, will be used to find the c_k coefficients required to update Eq. (6.3). Both the classical and modified Gram-Schmidt algorithms suffer from poor conditioning [28, 9]. We use the iterative modified Gram-Schmidt (IMGS) algorithm of Hoffman [28] (Ref. [28]’s “MGSCI” algorithm with $\kappa = 2$) for which Hoffmann conjectures an orthogonality relation $\|I - Q_k^T Q_k\|_2 \approx \kappa \epsilon_{\text{mach}} \sqrt{M}$. Orthogonalization of the j^{th} basis using Hoffman’s IMGS has an asymptotic FLOP count of $\mathcal{O}(\nu_j j N)$, where ν_j is the number of MGS iterations, which depends on j , and is typically less than 3. Fig. 6.1(b) (right) plots the scaled time T_j^{IMGS}/N with iteration index j for different values of N .

To summarize, our implementation of Alg. 3 requires $\mathcal{O}(2MNk + \frac{1}{2}\hat{\nu}Nk(k+1))$ operations to find k basis, where $\hat{\nu}$ is an “effective” value of ν_j .

Unless noted otherwise, our timing experiments have been carried out on either the San Diego Supercomputer Center’s machine Comet (each compute node features two Intel Xeon E5-2680v3 2.5 GHz chips, each equipped with 12 cores, and connected by an InfiniBand interconnect) or the National Center for Supercomputing Applications’ machine Blue Waters (each compute node features 32 OS-cores, and every 2 of these OS-cores share a single floating point unit. Nodes are connected by the Gemini interconnect). We have made only modest attempts at core-level optimization which, importantly, includes the use of Advanced Vector Extensions (AVX2) for vector-vector products.

6.1.3. Parallel code. We consider a natural parallelization-by-column strategy. Each core ² is given a subset of columns to manage, and a separate “master” core

²We consider parallelization with MPI (“by process”), OpenMP (“by thread”) and an MPI/OpenMP hybrid. To streamline the presentation, we avoid the terms “process” and “thread” in favor of “core”. Since we will never run more than one process or thread per core, the terminology should be unambiguous and clear from context. The book *Introduction to high performance computing for scientists and engineers* provides a comprehensive introduction to many of the high performance computing concepts discussed through this section [26].

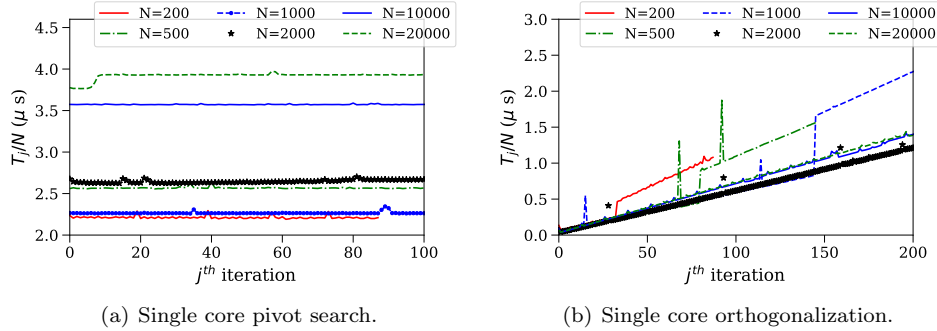


FIG. 6.1. **Left:** Pivot search time as a function of iteration index j . Based solely on operation counts one should expect T_j^{pivot}/N to be independent of N . Differences are likely due to data access latencies which do depend on N . **Right:** Orthogonalization time as a function of iteration index j . As expected, these quantities exhibit a linear growth with j . Timing data from the two smallest values of N “jump” due to additional orthogonalization iterations (ν increases from 1 to 2).

is responsible for all orthogonalization activities. We denote P_{pivot} as the number of cores devoted to the pivot search and P_{ortho} as the number of cores devoted to basis orthogonalization. Load balancing is trivially accomplished by distributing N/P_{pivot} columns of S among P_{pivot} cores. Each pivot core loads or creates its chunk of S in parallel. Parallelization of the orthogonalization portion of the algorithm will be discussed later; for now $P_{\text{ortho}} = 1$.

The j^{th} iteration is initiated after the orthogonalization core broadcasts the $j - 1$ basis vector to all P_{pivot} cores. Next, each pivot core computes its contribution of Eq. (6.3) and its maximum. This information is communicated to all pivot and orthogonalization cores. The pivot core with the global maximum residual error sends its column to the orthogonalization core to orthogonalize.

We model the j^{th} iteration’s computational cost as

$$T_j = T_j^{\text{pivot}} + T_j^{\text{IMGS}} + C_j, \quad (6.4)$$

where T_j^{IMGS} measures the orthogonalization time, T_j is the entire while loop appearing in Alg. 3, and C_j includes additional parallelization overheads such as any communication cost and/or thread-management overheads. As equality holds to at worst 1% (typically 0.001%), we often report only $T_j^{\text{pivot}} + C_j$ and T_j . All timing measurements are made from the master process, and the timer measuring T_j^{pivot} starts before the next basis vector is broadcasted to all the workers and ends after the next $j + 1$ (unorthogonalized) column basis has been received by the master process. Similar to the single core case (cf. Fig. 6.1(a)) we observe (as expected) $T_j^{\text{pivot}} + C_j$ to be independent of j and, therefore, often report values at some fixed value of j .

We consider parallelization by message passing interface (MPI) and OpenMP.

MPI. Each MPI process runs on a unique core. The pivot and orthogonalization cores communicate global pivot information using `MPI_Allreduce()`, the selected column vector is passed to the orthogonalization work using `MPI_Send()` and `MPI_BCast()` provides all the pivot cores with this new orthonormal basis³.

³We experimented with a few different MPI library functions, such as broadcast, reduction and

OpenMP. OpenMP uses threads to parallelize a portion of the code using the fork-join model. When using OpenMP, we define a large parallel region construct using P_{pivot} threads and enclosing the entire while loop; in fact most of the worker’s code is inside of the parallel region. We found this to give better performance results as compared with parallelizing the for-loop over columns, possibly because a wider parallelized region avoids multiple fork-joins. A designated master thread carries out the orthogonalization task.

Figure 6.2 considers a family of strong scaling tests where the matrix size is fixed and we vary the number of cores from 1 to 24. The left panel reports the parallelization efficiency

$$E_C = \frac{T_1}{CT_C}, \quad (6.5)$$

for the pivot search parallelized with OpenMP, where C is the number of cores, and T_1 and T_C denote the walltime using 1 and C cores, respectively. Perfect scalability is achieved whenever $E_C = 1$. The code’s speedup, another often quoted scalability measure, is simply $S_C = C \times E_C$.

Consistently high efficiencies are observed over a range of problem sizes, with speedups ≈ 20 routinely observed. For smaller problem sizes, the efficiency is reduced as the parallel overhead C_j becomes a sizable fraction of the overall cost⁴. Figure 6.2(a) shows the pivot search portion of the algorithm is efficiently parallelized. Figure 6.2(b) shows the full algorithm’s efficiency. Evidently scalability is poor for shorter matrices (small values of N), which should be expected from Eq. (6.4) and Amdahl’s law. Approximating the computational cost to be proportional to the asymptotic FLOP count and assuming $M \gg k$, $M > P_{\text{pivot}}k$ and $C_j = 0$, the efficiency of our algorithm is

$$E \approx 1 - \nu k(P_{\text{pivot}} - 1)/(2M). \quad (6.6)$$

Thus, for good scalability, our problem should require large values of M . Most model reduction applications easily meet this requirement. Indeed, model reduction seeks to approximate the underlying continuum problem (often with high parametric dimensionality) for which $M \rightarrow \infty$, while for parametrically smooth models $\sigma_k \propto \exp(-k)$. Together, these features suggest $M \gg kP_{\text{pivot}}$ is often satisfied in practice.

6.1.4. Large-core scaling. Our approach to distributed memory parallelization closely follows that of shared memory parallelization. As OpenMP does not support distributed memory environments we cannot use this library for inter-node communication. We consider two cases. First, a pure-MPI parallelization exactly as described in Sec. 6.1.3. Second, a hybrid MPI/OpenMP implementation launching one MPI process per socket⁵. In turn, each MPI process spawns a team OpenMP threads. Each thread is responsible for a matrix chunk over which a local pivot search is performed. As before we avoid multiple thread fork-joins by enclosing the entirety of the while-loop within an OpenMP parallel region, with the master thread responsible for all MPI calls (a so-called “funneled” hybrid approach). As only processes participate

gather, but found these to perform worst. The code’s git history documents these experiments, which are not reported here.

⁴Very large values of M , say $M \geq 10^6$, also shows reduced scalability presumably due to memory access times.

⁵To improve memory access performance, all MPI processes and their threads are bound to a socket.

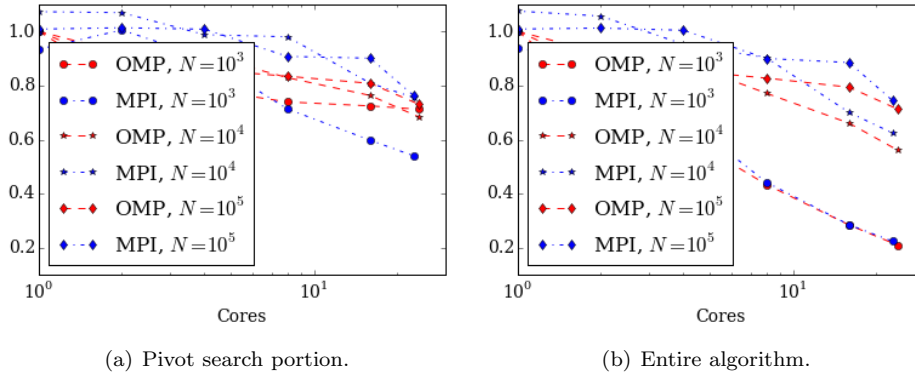


FIG. 6.2. Strong scaling efficiency versus cores for a sequence of increasingly “tall” matrices with $M = 1,000$ and $k = 100$ fixed. Our tests were performed on a 24-core shared memory node of the supercomputer Comet. Blocks of columns are distributed to each core with increasingly fewer blocks per core. Specifically 1000, 500, 250, 125, 62, and 43 columns are distributed among, respectively, 1, 2, 4, 8, 16 and 24 cores. We measure scalability for the pivot search portion (from the timing data T_{pivot}) of the algorithm (left) and the full algorithm (right).

in inter-node communication, a hybrid code potentially reduces the communication overhead as compared to a pure-MPI implementation. These benefits could become increasingly important at extremely large core counts.

Figure 6.3 reports on a few scalability tests we ran on Comet. First, we consider how the pivot search portion of the algorithm scales to large core counts for a fixed matrix size. Figure 6.3(a) shows a typical case. We see that going from one core to one node maintains high efficiencies, which should be expected in light of Fig. 6.2(a). Running on an increasing number of cores means each core has less work to do (fewer columns per core) while the entire algorithm has more communication. As expected, the efficiency decreases but maintains high values up to 370 cores. Such observations are matrix-dependent, and larger (smaller) matrices are expected to exhibit better (worse) scalability. Interestingly, the MPI/OpenMPI hybrid strategy performs much better than pure-MPI for this problem, indicating that the communication overhead can be somewhat ameliorated; this is also a matrix-dependent observation. Next, we consider how the entire algorithm scales to large core counts when the matrix size is also increased commensurate to the number of core; this constitutes a weak scaling test. Figure 6.3(b) shows a typical case. We see that the full program’s runtime has negligible increase when going from one core to 1,728 cores (the maximum allowable size on Comet). This demonstrates that very large matrices can be efficiently handled.

As a final demonstration of our code’s capabilities, we repeat the weak scaling test on Blue Waters where more cores can be used. Figure. 6.4 shows the same excellent weak scalability all the way up to 32,768 cores. In particular, we perform a column pivoted QR decomposition (to discover the first $k = 100$ basis) on a 10,000-by-3,276,800 sized matrix in 13.5 seconds. For comparison, it took a similar time of 11.5 seconds to QR decompose a much smaller 10,000-by-3,200 matrix using 32 cores.

6.1.5. Discussion and Limitations. We have demonstrated our code is capable of handling very large matrix sizes. For smaller sized matrices, the orthogonalization routine becomes a performance obstacle. Because the basis is revealed

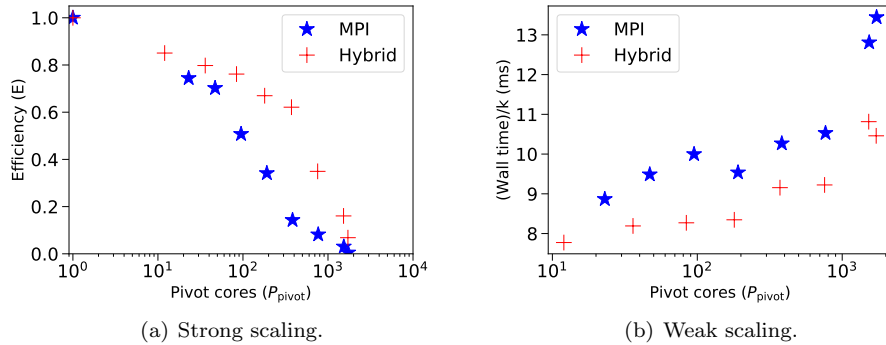


FIG. 6.3. Scalability on the supercomputer Comet up to 1,728 cores with $k = 100$. **Left:** Strong scaling efficiency of the pivot search part of the algorithm for a matrix with $N = 1,000$ rows and $M = 240,000$ columns. At 1728 cores, each pivot core has ≈ 138 columns and the MPI (Hybrid) efficiency is .005 (.07), corresponding to very small speedups. This is expected; at this scale the communication time is a sizable fraction of the overall cost, and only increasing the workload (more rows or columns) would increase the efficiency. For this particular matrix size, using 370 cores the hybrid parallelization strategy has good efficiencies of about .62. Of particular importance is that the hybrid code is significantly more efficient than the pure-MPI code. **Right:** Weak scaling efficiency of the full algorithm for a matrix with $N = 10,000$ rows and $M = P_{\text{pivot}} \times 100$ columns. The total time is scaled by $k = 100$. The slow growth in the total time with increasingly more cores/columns demonstrates good weak scalability, allowing very large matrices to be tackled. (perfect weak scalability would result in a horizontal line.)

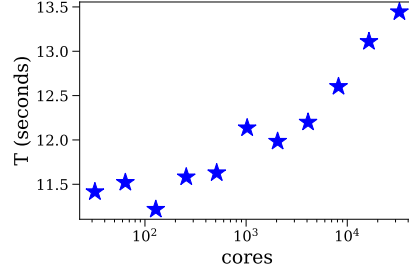


FIG. 6.4. Weak scaling on Blue Waters with $N = 10,000$ rows and $k = 100$. We let the number of columns $M = 100 \times \text{cores}$ scale linearly with the number of cores. The number of cores is increased from 32 to 32,768, with the largest matrix having 3,276,800 columns. A mild logarithmic growth in the full algorithm's time is evident, and the good weak scalability demonstrates the ability to compute column pivoted QR decompositions of extremely large matrices.

sequentially, certain efficient algorithms (such as block QR) are not applicable [22]. Furthermore, for conditioning purposes, we have used the IMGS of Hoffman which cannot be written as a matrix-vector product when the basis are sequentially known, thereby precluding efficient BLAS-2 routines [22]. Briefly, we offer three potential solutions. First, alternative orthogonalization algorithms, like the “CMGSI” algorithm of Hoffman may be better suited for parallelization [28]. Second, specialized accelerator hardware may reduce the vector-vector product costs by offloading. Finally, one could consider alternative global pivot selection criteria by overlapping the pivot search and orthogonalization computations.

7. Concluding remarks. Dimensional and model-order reduction have a wide range of applications. In this paper, we have considered two of the most popular dimensional-reduction algorithms, SVD and QR decompositions, and summarized their most important properties. In most model-based dimensional reduction applications the model varies smoothly with parameter variation. In such cases, matrices like the Kahan one are rarely (if ever) encountered in practice. Instead, the approximation problem is characterized by a fast decaying Kolmogorov n -width. Due to the equivalence we showed between the RB-Greedy algorithm and a certain QR pivoting strategies, we argue that, for many cases, a QR-based model reduction approach is preferable to an SVD-based one. The QR decomposition is faster and more easily parallelized while providing comparable approximation errors.

Finally, we have described a new, publicly-available QR-based model reduction code, `greedycpp` [1]. Our code is based on a well-conditioned version of the MGS algorithm which overcomes the stability issues which plague ordinary GS while being straightforward to parallelize (as compared to Householder reflections or Givens rotations). This massively parallel code, developed with model reduction in mind, performed QR decomposition on matrices as large as 10,000-by-3,276,800 on the supercomputers Comet and Blue Waters. Parts of this code have been used to accelerate gravitational wave inference problems [37, 12, 2, 3].

Acknowledgments. We acknowledge helpful discussions with Yanlai Chen, Howard Elman, Chad Galley, Frank Herrmann, Alfa Heryudono, Saul Teukolsky, and Manuel Tiglio. We thank Priscilla Canizares, Collin Capano, Peter Diener, Jeroen Meidam, Michael Purrer, Rory Smith, and Ka Wa Tsang for careful error reporting, code improvements and testing of early versions of the `greedycpp` code. Michael Purrer and Rory Smith for interfaces to the gravitational waveform models implemented in LAL-Simulation. SEF was partially supported by NSF award PHY-1606654 and the Sherman Fairchild Foundation. HA was partially supported by NSF grant DMS-1521590. Computations were performed on NSF/NCSA Blue Waters under allocation PRAC ACI-1440083, on the NSF XSEDE network under allocations TG-PHY100033 and TG-PHY990007, and on the Caltech compute cluster Zwicky (NSF MRI-R² award no. PHY-0960291).

REFERENCES

- [1] <https://bitbucket.org/sfield83/greedycpp>.
- [2] BP ABBOTT, R ABBOTT, TD ABBOTT, MR ABERNATHY, F ACERNESE, K ACKLEY, C ADAMS, T ADAMS, P ADDESSO, RX ADHIKARI, ET AL., *First search for gravitational waves from known pulsars with advanced ligo*, The Astrophysical Journal, 839 (2017), p. 12.
- [3] BENJAMIN P ABBOTT, R ABBOTT, TD ABBOTT, F ACERNESE, K ACKLEY, C ADAMS, T ADAMS, P ADDESSO, RX ADHIKARI, VB ADYA, ET AL., *Gw170814: A three-detector observation of gravitational waves from a binary black hole coalescence*, Physical Review Letters, 119 (2017), p. 141101.
- [4] ———, *Gw170817: observation of gravitational waves from a binary neutron star inspiral*, Physical Review Letters, 119 (2017), p. 161101.
- [5] B. P. ABBOTT AND ET AL., *Gw170104: Observation of a 50-solar-mass binary black hole coalescence at redshift 0.2*, Phys. Rev. Lett., 118 (2017), p. 221101.
- [6] H. ANTIL, S. E. FIELD, F. HERRMANN, R. H. NOCHETTO, AND M. TIGLIO, *Two-step greedy algorithm for reduced order quadratures*, J. Sci. Comput., 57 (2013), pp. 604–637.
- [7] P. BINEV, A. COHEN, W. DAHMEN, R. DEVORE, G. PETROVA, AND P. WOJTASZCZYK, *Convergence rates for greedy algorithms in reduced basis methods*, SIAM J. Math. Anal., 43 (2011), pp. 1457–1472.
- [8] C. H. BISCHOF, *A parallel qr factorization algorithm with controlled local pivoting*, SIAM Journal on Scientific and Statistical Computing, 12 (1991), pp. 36–57.

- [9] Å. BJÖRCK, *Solving linear least squares problems by Gram-Schmidt orthogonalization*, Nordisk Tidskr. Informations-Behandling, 7 (1967), pp. 1–21.
- [10] A. BUFFA, Y. MADAY, A. T. PATERA, C. PRUD'HOMME, AND G. TURINICI, *A priori convergence of the greedy algorithm for the parametrized reduced basis method*, ESAIM Math. Model. Numer. Anal., 46 (2012), pp. 595–603.
- [11] P. BUSINGER AND G. H. GOLUB, *Handbook series linear algebra. Linear least squares solutions by Householder transformations*, Numer. Math., 7 (1965), pp. 269–276.
- [12] P. CANIZARES, S. E. FIELD, J. GAIR, V. RAYMOND, R. SMITH, AND M. TIGLIO, *Accelerated gravitational wave parameter estimation with reduced order modeling*, Physical review letters, 114 (2015), p. 071104.
- [13] T. F. CHAN, *Rank revealing QR factorizations*, Linear Algebra Appl., 88/89 (1987), pp. 67–82.
- [14] T. F. CHAN AND P. C. HANSEN, *Some applications of the rank revealing QR factorization*, SIAM J. Sci. Statist. Comput., 13 (1992), pp. 727–741.
- [15] S. CHANDRASEKARAN AND I. C. F. IPSEN, *On rank-revealing factorisations*, SIAM J. Matrix Anal. Appl., 15 (1994), pp. 592–622.
- [16] S. CHATURANTABUT AND D. C. SORENSEN, *Nonlinear model reduction via discrete empirical interpolation*, SIAM Journal on Scientific Computing, 32 (2010), pp. 2737–2764.
- [17] P. G. CONSTANTINE, D. F. GLEICH, Y. HOU, AND J. TEMPLETON, *Model reduction with mapreduce-enabled tall and skinny singular value decomposition*, SIAM Journal on Scientific Computing, 36 (2014), pp. S166–S191.
- [18] J. W. DEMMEL, L. GRIGORI, M. GU, AND H. XIANG, *Communication avoiding rank revealing QR factorization with column pivoting*, SIAM J. Matrix Anal. Appl., 36 (2015), pp. 55–89.
- [19] R. DEVORE, G. PETROVA, AND P. WOJTASZCZYK, *Greedy algorithms for reduced bases in Banach spaces*, Constr. Approx., 37 (2013), pp. 455–466.
- [20] Z. DRMAČ AND Z. BUJANOVIĆ, *On the failure of rank-revealing QR factorization software—a case study*, ACM Trans. Math. Software, 35 (2009), pp. Art. 12, 28.
- [21] S. E. FIELD, C. R. GALLEY, AND E. OCHSNER, *Towards beating the curse of dimensionality for gravitational waves using reduced basis*, Physical Review D, 86 (2012), p. 084046.
- [22] E. GALLOPOULOS, B. PHILIPPE, AND A. H. SAMEH, *Parallelism in matrix computations*, Scientific Computation, Springer, Dordrecht, 2016.
- [23] L. GIRAUD, J. LANGOU, M. ROZLOŽNÍK, AND J. VAN DEN ESHOF, *Rounding error analysis of the classical Gram-Schmidt orthogonalization process*, Numer. Math., 101 (2005), pp. 87–100.
- [24] G. GOLUB, *Numerical methods for solving linear least squares problems*, Numer. Math., 7 (1965), pp. 206–216.
- [25] G. H. GOLUB AND C. F. VAN LOAN, *Matrix computations*, Johns Hopkins Studies in the Mathematical Sciences, Johns Hopkins University Press, Baltimore, MD, third ed., 1996.
- [26] G. HAGER AND G. WELLEIN, *Introduction to high performance computing for scientists and engineers*, CRC Press, 2010.
- [27] M. HANNAM, P. SCHMIDT, A. BOHÉ, L. HAEGEL, S. HUSA, F. OHME, G. PRATTEN, AND M. PÜRRER, *Simple model of complete precessing black-hole-binary gravitational waveforms*, Phys. Rev. Lett., 113 (2014), p. 151101.
- [28] W. HOFFMANN, *Iterative algorithms for Gram-Schmidt orthogonalization*, Computing, 41 (1989), pp. 335–348.
- [29] Y. P. HONG AND C.-T. PAN, *Rank-revealing QR factorizations and the singular value decomposition*, Math. Comp., 58 (1992), pp. 213–232.
- [30] S. HUSA, S. KHAN, M. HANNAM, M. PÜRRER, F. OHME, X. J. FORTEZA, AND A. BOHÉ, *Frequency-domain gravitational waves from nonprecessing black-hole binaries. I. New numerical waveforms and anatomy of the signal*, Phys. Rev., D93 (2016), p. 044006.
- [31] S. KHAN, S. HUSA, M. HANNAM, F. OHME, M. PÜRRER, X. J. FORTEZA, AND A. BOHÉ, *Frequency-domain gravitational waves from nonprecessing black-hole binaries. II. A phenomenological model for the advanced detector era*, Phys. Rev., D93 (2016), p. 044007.
- [32] Y. MADAY, N. C. NGUYEN, A. T. PATERA, AND S. H. PAU, *A general multipurpose interpolation procedure: the magic points*, Communications on Pure and Applied Analysis, 8 (2009), pp. 383–404.
- [33] JEROEN MEIDAM, KA WA TSANG, JANNA GOLDSTEIN, MICHALIS AGATHOS, ARCHISMAN GHOSH, CARL-JOHAN HASTER, VIVIEN RAYMOND, ANURADHA SAMAJDAR, PATRICIA SCHMIDT, RORY SMITH, ET AL., *Parametrized tests of the strong-field dynamics of general relativity using gravitational wave signals from coalescing binary black holes: Fast likelihood calculations and sensitivity of the method*, Physical Review D, 97 (2018), p. 044033.
- [34] A. PINKUS, *N-widths in Approximation Theory*, Springer-Verlag, 1985.
- [35] G. QUINTANA-ORTÍ AND E. S. QUINTANA-ORTÍ, *Parallel Algorithms for Computing Rank-Revealing QR Factorizations*, Springer Berlin Heidelberg, Berlin, Heidelberg, 1997,

- pp. 122–137.
- [36] A. RUHE, *Numerical aspects of gram-schmidt orthogonalization of vectors*, Linear Algebra and its Applications, 5253 (1983), pp. 591 – 601.
 - [37] R. SMITH, S. E. FIELD, K. BLACKBURN, C.-J. HASTER, M. PÜRRER, V. RAYMOND, AND P. SCHMIDT, *Fast and accurate inference on gravitational waves from precessing compact binaries*, Physical Review D, 94 (2016), p. 044031.
 - [38] D. B. SZYLD, *The many proofs of an identity on the norm of oblique projections*, Numer. Algorithms, 42 (2006), pp. 309–323.
 - [39] L. N. TREFETHEN AND D. BAU, III, *Numerical linear algebra*, Society for Industrial and Applied Mathematics (SIAM), Philadelphia, PA, 1997.
 - [40] J. A. TROPP, *Column subset selection, matrix factorization, and eigenvalue optimization*, in Proceedings of the Twentieth Annual ACM-SIAM Symposium on Discrete Algorithms, Society for Industrial and Applied Mathematics, 2009, pp. 978–986.
 - [41] J. XU AND L. ZIKATANOV, *Some observations on Babuška and Brezzi theories*, Numer. Math., 94 (2003), pp. 195–202.